Numerical and conceptual evaluation of preferential flow in Zarqa River Basin, Jordan

Michel Rahbeh [a,*], Raghavan Srinivasan [b], Rabi Mohtar [b]

[a] University of Jordan, Faculty of Agriculture, Department of Land, Water and Environment, Jordan
[b] Texas A&M University, United States

A R T I C L E I N F O

A B S T R A C T

Farmers along the main reach of the Zarqa River Basin (ZRB) commonly utilize treated wastewater for irrigation. Deep percolation is expected to occur as a result of irrigation, and it is expected that preferential flow pathways may facilitate the downward movement of irrigation water. Therefore, the aim of this research was to investigate the susceptibility of soils near Zarqa River to preferential flow, and the HYDRUS and Soil and Water Assessment Tool (SWAT) models were used. The methodology consisted of taking tension infiltrometer measurements along the Zarqa River to determine the main physical properties relevant to preferential flow, such as infiltration rate and macroscopic capillary length, followed by investigating the downward water movement using HYDRUS and SWAT. The HYDRUS simulations were conducted using single porosity (SP) and dual porosity (DP) constitutive functions pertaining to matrix and preferential flow, respectively. The in situ tension infiltrometer measurements were used to parameterize the surface layer of the HYDRUS DP model. HYDRUS simulations showed that preferential flow occurring in the surface layer of the soil profile controlled the vertical movement of soil water in excess of field capacity. The comparison between SWAT, SP and DP showed that both SWAT and DP were capable of simulating preferential flow in arid watersheds. However, SWAT simulations of lateral discharge and deep percolation resemble that of the DP only when the evaporation soil compensation factor (ESCO) was set to a value of 0.8 and the length of the soil slope was set to its maximum value. This research recommends using HYDRUS model to verify SWAT model predictions of soil water redistribution in the soil profile and to improve the parameterization of the SWAT model. The research also suggests an approach for the combined use of both models.

1. Introduction

Preferential water flow movement is a natural phenomenon that occurs in most soils, and it has been widely recognized as the major contributor to deep percolation and subsequent groundwater recharge (Hatiye et al., 2017; Vásquez et al., 2015). The preferential flow process has been identified on the local and field scales through in situ measurements and the use of tracers. Field observations showed high variability of preferential flow both in magnitude and mode of occurrence (Wiekenkamp et al., 2016; Sheng et al., 2012; Hardie et al., 2011; Wang and Zhang, 2011). Despite the variability in preferential flow, HYDRUS provided satisfactory predictions for solute transport in soil columns with artificially configured macro-pores (Xu et al., 2017; Wang et al., 2014). HYDRUS is a three dimensional (3D) numerical model that

* Corresponding author.
E-mail addresses: m.rahbeh@ju.edu.jo (M. Rahbeh),
srinivasan@tamu.edu (R. Srinivasan), mohtar@aub.edu.lb (R. Mohtar).

simulates saturated and unsaturated soil water movement and redistribution. HYDRUS uses a finite element scheme to solve Richard's equation in single or dual permeability domains. The model is equipped with a user-friendly interface that allows the handling of homogenous or heterogeneous problem domains and accommodates complex geometries. The constitutive equations that account for unsaturated hydraulic conditions in a single permeability domain were described by van Genuchten (1980) (VG equations), Brooks and Corey (1964), and Vogel and Císlerová (1988), who described modified VG equations. These equations describe the unsaturated hydraulic conditions in a single pore space (single porosity; henceforth SP). The single permeability domain in HYDRUS model also includes constitutive equations that accommodate porous media of two overlapping pore spaces (dual porosity; henceforth DP). In contrast with the single permeability domain, the dual permeability model enables HYDRUS to simulate water flow in fracture and matrix domains (Šimůnek et al., 2016).

Among the many uses of HYDRUS there are enhanced determination of soil physical characteristics from field measurements (Bordoni et al., 2017; Cong et al., 2014; Antonopoulos et al., 2013), determination of soil water dynamics (Wegehenkel et al., 2017; Li et al., 2015), and evaluation of groundwater recharge (Wu et al., 2016). HYDRUS has also been used to simulate interactions between soil and groundwater, as well as the impact of irrigation practices on return flow and contaminant transport to groundwater (Hu et al., 2017; Shang et al., 2016).

Although diverse in scope, the HYDRUS model is confined to small scales and is not suitable for evaluating soil water movement at the watershed scale. The Soil and Water Assessment Tool (SWAT) is more commonly used for evaluation of water and environmental problems in mid-sized to large catchments (Gassman et al., 2007). SWAT is a conceptual hydrological model based on the soil water balance equation. The change in soil water storage in any given time step is determined by the net difference between precipitation and other components of the hydrological cycle including evapotranspiration, lateral subsurface discharge to the main reach, surface runoff and deep percolation. A SWAT model setup may consist of several sub-watersheds, and each sub-watershed is divided into different Hydrological Response Units (HRUs). The soil water balance equation is solved for each HRU, so the HRU is the basic simulation unit in SWAT. Each HRU is defined by a unique set of parameters. SWAT also incorporates a comprehensive set of hydrological and hydraulic functions that account for streamflow and sediment routing between sub-watersheds, and the influence of management practices. SWAT also allows interaction between surface water and groundwater (Arnold et al., 1998).

Recent implementations of SWAT have mainly been focused on evaluation of the impact of irrigation, urbanization, and changes in agricultural land use on watershed hydrological pathways (Hartwich et al., 2016; Neupane and Kumar, 2015; Rahbeh et al., 2013). Another major area of SWAT utilization is assessment of short- and long-term climate change impacts on water yield (Neupane et al., 2015; Musau et al., 2015; Narsimlu et al., 2013).

Indeed, SWAT can be instrumental to planning present and future watershed management activities.

However, some important environmental processes occurring at the field and farm scales may not be well represented in the SWAT model, especially in arid areas where the annual rainfall is not sufficient to produce substantial runoff (Cho et al., 2009). Studies conducted by Al-wadaey et al. (2016) and Ouessar et al. (2009) highlight another hurdle of implementing SWAT in arid regions. Both studies showed the potential of SWAT to pinpoint ideal locations for introducing conservation practices and water harvesting structures. However, due to scarcity of runoff data, they were unable to conduct a standard calibration–validation procedure. Instead, they validated their model by relying on expert knowledge and comparisons with a limited number of runoff measurements. The lack of observed data at the study watershed prompted Taddele et al. (2016) to calibrate and validate SWAT on a watershed encompassing the study watershed. Then, the optimized parameters were transferred into the SWAT model developed for the study watershed. For an agricultural watershed that hardly produced any runoff, Awan and Ismaeel (2014) calibrated and validated SWAT by contrasting the SWAT simulated evapotranspiration (ET) with the ET determined by the surface energy balance algorithm (SEBAL). The calibrated SWAT model was then used to assess groundwater recharge. Ahn et al. (2018) studied the impact of drought on irrigation practices in an arid watershed where runoff was minimal, hence 90% of the streamflow originated from a reservoir located upstream of the watershed inlet. Also, streamflow tended to dwindle in the downstream direction due to withdrawals of irrigation water from the main reach. Nevertheless, Ahn et al. (2018) successfully used the SWAT model to simulate the impact of irrigation on the main hydrological components within the study watershed.

Zarqa River Basin (ZRB) is one of the most important basins in Jordan; it is the home of half the Jordanian population and also supplies the farmers of the Jordan Valley with irrigation water. It drains an area of approximately 3900 km^2 into the King Talal Dam (KTD). Most of the runoff water originates from the northwestern part of the watershed, where the long-term annual rainfall is approximately 650 mm. The average annual rainfall generally decreases rapidly in the north-to-south and west-to-east directions and drops below 100 mm in the eastern part of the watershed. One of the main concerns about the ZRB is that preferential flow and transport may be occurring in the cultivated areas along the main reach of the river. Similar to the case study presented by Ahn et al. (2018), farmers draw irrigation water directly from the river or from groundwater wells adjacent to the river. The groundwater level is increasing by an average of 20 cm per year (Bajjali et al., 2017), as the groundwater is recharged from the river bed and irrigated areas. The rise of the groundwater level raises the concern that water and solutes move faster than anticipated through preferential pathways that can potentially occur in soils located around the main reach (Al-Kuisi et al., 2014). The average annual rainfall in the cultivated areas along the Zarqa River is less than 150 mm. Consequently, because of the minimal anticipated runoff generation from this area, its relative

importance can be easily underestimated for a model calibrated to streamflow data. Therefore, downscaling from the watershed scale to the farm scale is necessary for proper assessment of hydrological processes occurring at local scales. In this regard, HYDRUS can be a useful tool for in-depth assessment and improvement of SWAT handling of preferential flow.

This study aims to investigate the (1) influence of preferential flow on the vertical and lateral redistribution of water in soil adjacent to Zarqa River using the HYDRUS model, and (2) the ability of the SWAT model to predict preferential flow in a selected sub-watershed within the study area.

2. Methodology

2.1. Study area

The area adjacent to the main reach of Zarqa River (henceforth "study area") extends between the Khirbat Es-
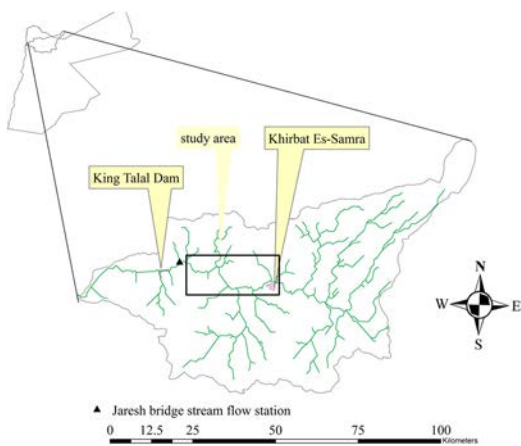

Fig. 1. The location of the study area within the Zarqa River Basin. The study area (indicated by the rectangular box) is located between the Khirbat Es-Samra treatment plant (KTP) and the King Talal Dam (KTD) and is adjacent to the main reach.

Samra treatment plant (KTP) and the KTD (Fig. 1), and it is cultivated with forage crops and vegetables as well as olive and citrus orchards. A land use map for the entire ZRB is available (Al-Bakri et al., 2013). Irrigated areas constitute 7% of the ZRB, while rainfed barley, urban areas, mixed agricultural areas, sparsely vegetated areas, and gravel plains constitute 8, 11, 16, 24 and 28% of the ZRB, respectively. However, the land use data of the study area were refined based on Landsat Images covering the period from September 2013 to September 2014. The red and near infrared bands of the Operational Land Imager (OLI) of Landsat 8 were processed to derive multi-temporal images of the normalized difference vegetation index (NDVI) (Fig. 2).

Daily discharge records for the KTP are available from 1986 to 2010 (Water Authority of Jordan, unpublished data files). From January 2000 to December 2009, KTP provided an average daily discharge of 1.5×10^5 m^3 of reclaimed water. However, in 2010 the average daily discharge increased to 1.77×10^5 m^3. A significant portion of the KTP outflow is used to irrigate the agricultural lands adjacent to the main reach of the Zarqa River. The farm land is 300–500 m above sea level, and characterized by fertile loamy soils with 1.5–3% organic content (Table 1). The relatively warm weather with an average temperature of approximately of 19 °C enables intensive farming. The average rainfall depth of about 132 mm provides only a small fraction of total crop water requirements, so the agricultural practices are mainly dependent on irrigation water from the river or local wells. As water is readily available, farmers tend to over irrigate their crops.

2.2. Climatic record

Rainfall data were requested directly from the Jordanian Ministry of Water and Irrigation (MWI). The unpublished database of the MWI contains rainfall records from 56 stations distributed throughout the ZRB. Other forms of climate data such as wind speed, sunshine hours, solar radiation and temperature were acquired from the Climate Forecast Reanalysis System (CFSR, 2014).
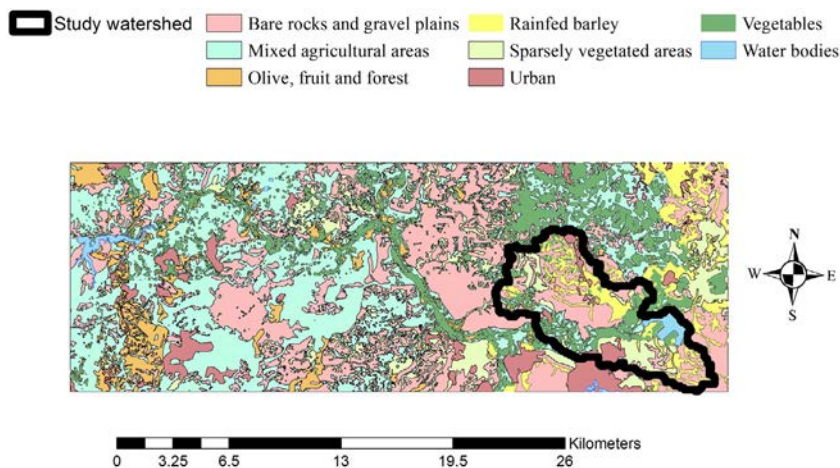

Fig. 2. The land uses in the study area and the delineated SWAT watershed. The land use map is based on the work of Al-Bakri et al. (2013) and is refined using Landsat images covering the period from September 2013 to September 2014.

Table 1
Description of the soil units encountered in the SWAT watershed (MOA, 1994). SOM denotes soil organic matter. The %CaCO$_3$ values are reported from soil sample analysis conducted by the research team.

Soil unit	Name	Sub group	Texture	Depth (m)	Porosity (%)	SOM	%CaCO3
AYD/8	Aydoun	Typic Xerochrepts	Silty clay loam	1.42	50	3.9	47
Tha/15	Ramtha	Xerochreptic Camborthids	Clay loam	0.86	44	1.8	42
NIS/11	Nisab	Xerochreptic Camborthids	Silt loam	0.48	44	1.5	37

Daily rainfall was collected from the Hashimiya station, located at 32°08′07.7″ N 36°06′47.4″ E, approximately 1800 m from the selected site for HYDRUS modeling (henceforth "HYDRUS site") (Fig. 3). The station provides over 30 years of recorded data. Temperature, solar radiation, and sunshine hours were collected from a grid point (CFSR, 2014) located at 32°00′14.4″ N 35°56′16.8″ E, approximately 20 km from the HYDRUS site. Fig. 4 shows considerable variability in annual rainfall, ranging from 42 to 245.9 mm. The maximum rainfall of 245.9 mm occurred in 1992 and was preceded by near average rainfall of 158.2 mm in 1991 and below average rainfall of 94.5 mm in 1990. Also, it was followed by an extreme low annual rainfall of 47 mm in 1993. Since the period from 1990 to 1993 represents heterogeneous climate conditions including low to maximum annual rainfall, the comparison between HYDRUS and SWAT models was conducted

Fig. 3. The soil map for the SWAT watershed. Also shown are the distribution of macro-porosity, the Zarqa River Basin, location of the HYDRUS site, and the location of the Hashimiya rainfall gauge.

Fig. 4. Annual rainfall observed at the Hashimiya rainfall station (32°08′07.7″ N 36°06′47.4″ E).

during the period (henceforth "simulation period") between January 1st 1990 and December 31st 1993.

2.3. Site measurements

In situ measurements of the soil physical properties of the surface layer along the Zarqa River were conducted using a standard tension infiltrometer equipped with a pressure transducer and a data logger (supplied by ICT international), similar to the device described by Ankeny et al. (1988). The measured soil properties include macroscopic capillary length and infiltration rate. The in situ tension infiltrometer measurements were conducted at 73 locations. The measurements at each location were conducted at tensions of −6, −3, and 0 cm. The infiltration at each tension was maintained until a steady-state condition was attained. The measurement time varied between 20 to 90 minutes depending on the soil type. The macroscopic capillary length was determined using Wooding's equation (1968):

$$Q(h_i) = \pi r^2 K_s \exp(\alpha h_i)\left(1 + \frac{4}{\pi r \alpha}\right) \tag{1}$$

where $Q(h_i)$ is the flow rate at tension h_i (L^3/T), K_s is the saturated hydraulic conductivity (L/T), α is the inverse macroscopic capillary length (1 L^{-1}), and r is the radius of the tension infiltrometer disk (L).

Based on the work of White and Sully (1987), a macroscopic capillary length of less than 80 mm was considered an indication of preferential flow. The macroscopic capillary length values (Fig. 3) showed that most soils along the Zarqa River are susceptible to preferential flow, especially in the vicinity of KTP. Therefore, the HYDRUS site was selected downstream of KTP for further investigation of soil water redistribution and downward movement using HYDRUS and subsequent comparison with SWAT model simulations (Fig. 3). It was delineated based on land use boundaries. It is cultivated with vegetables (cauliflower, lettuce, and cabbage) and characterized by steep slopes.

The HYDRUS site comprises a relatively small area of 70,160 m^2 and cannot be delineated as a watershed. To enable comparisons between HYDRUS and SWAT, an on-stream watershed (henceforth "SWAT watershed"), defined by an inlet and an outlet that encompasses the HYDRUS site was delineated along the main reach (Fig. 3). Fig. 3 shows that there are three types of soils in the watershed (MOA, 1994). These are (i) AYD/8 (Aydoun), characterized by a soil depth of approximately 142 cm and a silt clay texture; (ii) NIS/II (Nisab), a silt loam soil with a shallow soil profile of 48 cm; and (iii) Tha/15 (Ramatha) with a clay loam texture and a depth of 86 cm. The soils in
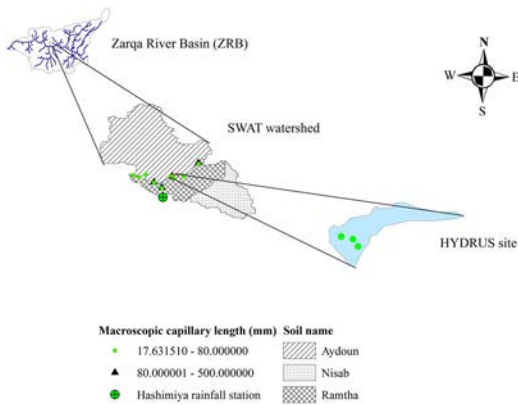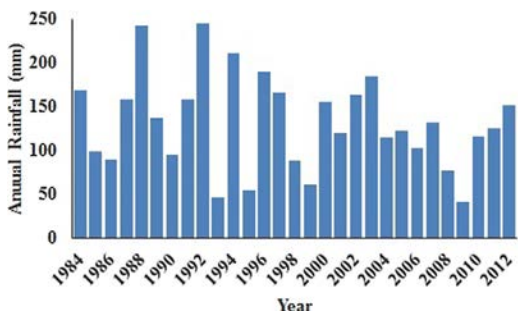
the SWAT watershed belong to Typic Xerochrepts and Xerochreptic Camborthids subgroups (Table 1).

2.4. SWAT model

2.4.1. General description

SWAT uses a simplified soil physical characterization based mainly on the available soil water content (AWC) defined as the difference between permanent wilting point and field capacity. If the soil water content within the soil profile exceeds the field capacity, then the excess water goes to deep percolation according to the following routing model (Neitsch et al., 2002):

$$w_{perc,ly} = SW_{ly,excess} \cdot \left(1 - \exp\left[\frac{-\Delta t}{TT_{perc}}\right]\right) \quad (2)$$

where $w_{perc,ly}$ is the amount of water percolating to the underlying soil layer, and $SW_{ly,excess}$ is the drainable volume of water in soil layer on a given day.

The travel time TT_{perc} is calculated on a daily basis for each soil layer:

$$TT_{perc} = \frac{SAT_{ly} - FC_{ly}}{K_{sat}} \quad (3)$$

Root distribution influences the actual transpiration and redistribution of soil water. Typically, the maximum root density is located near the surface and decreases vertically. In SWAT this distribution is handled by the following function (Neitsch et al., 2002):

$$w_{uptake} = \frac{PT_t}{1 - e^{-B_w}} \cdot \left[1 - e^{-B_w \cdot \frac{z}{z_{root}}}\right] \quad (4)$$

where w_{uptake} (mm) is the root water uptake, PT_t (mm) is the potential transpiration, z (mm) is the potential water uptake from the soil surface to specified depth, z_{root} (mm) is the maximum rooting depth, and B_w is the water use

distribution parameter. This parameter is set to 10 (its default value in SWAT model), which means that 50% of water uptake will occur from the upper 6% of the root zone.

2.4.2. Setup of the SWAT model for SWAT watershed

The land use map, soil map and four slope classes (0–5, 5–10, 10–15, and 15–9999%) were overlaid using threshold values of 8, 8, and 0% for land use, soil, and slope classes, respectively. Overall, SWAT generated 38 HRUs for the SWAT watershed. The two soil types within the HYDRUS site are associated with four slope classes distributed over seven HRUs (Table 3). The results of the SWAT model were expressed as the area weighted averages of the HRU outputs. For SWAT initialization, the simulation period (January 1st, 1990 – December 31st, 1993) was preceded by a warm-up period that started on January 1st, 1984 and ended on December 31st, 1989. A daily time step was used for all SWAT runs.

2.4.3. Parameterization of SWAT model for SWAT watershed

The premise of this study is to downscale from the watershed scale to the local scale. That would enable assessing and enhancing SWAT handling of the processes occurring at the local scale. The HYDRUS model can be used to assess the soil water redistribution within the soil profile. Then the results of the HYDRUS model can be compared with the output produced by the SWAT model. Meaningful comparison between the two models requires matching parameterization. The saturated hydraulic conductivity, bulk density and soil texture in the SWAT model should reflect their counterpart values in HYDRUS model. Also, a full calibration for the soil properties of the SWAT model requires continuous monitoring of the soil water content, which is not practically possible. Therefore, both models were parameterized based on prior knowledge deduced from the soil maps and in situ soil measurements (Table 2).

Table 2

Soil physical characteristics of two soil types occurring within the HYDRUS site. The soil physical properties of the surface layer were derived from the tension infiltrometer measurements and the soil map. Q_r is the residual soil water content (m³/m³), Q_s is the saturated soil water content (m³/m³), α (1 m^{-1}) and n are fitting parameters of the soil water retention function for the main region (Eq. (5)) or the first region in the case of Eq. (7), α^2 (1 m^{-1}) and n^2 – fitting parameters of the second region (Eq. (7)), and w – the weighting factor for the second region of Eq. (7).

Depth (mm)	Clay %	Silt	Sand	Q_r (1 m^{-1})	Q_s	α (m/day)	n	K_s (1 m^{-1})	w	α^2	n^2
Soil physical parameters of shoulder slope (Aydoun)											
Dual porosity parameters for the surface layer											
320	15	16.8	68.2	0.051	0.3819	1.68	1.1832	0.6905	0.15283	18.559	3.902
Single porosity parameters											
320	15	16.8	68.2	0.053	0.3819	3.13	1.388	0.3219			
870	42.7	37.7	19.6	0.093	0.4726	1.33	1.3543	0.1286			
1420	49.4	39.7	6.90	0.101	0.4968	1.44	1.3204	0.1817			

Depth (mm)	Clay %	Silt	Sand	Q_r (1 m^{-1})	Q_s	α (m/day)	n	K_s (1 m^{-1})	w	α^2	N^2
Soil physical parameters of the back slope Tha/15											
Dual porosity parameters for the surface layer											
320	6.8	30	63.2	0.035	0.3906	2.14	1.101	0.546	0.26	6.8E–05	1.001
Single porosity parameters											
320	6.8	30	63.2	0.035	0.3906	2.92	1.041	0.4978			
590	24.9	56.2	18.9	0.096	0.4851	1.10	1.422	0.1331			
870	39.8	48.2	12.0	0.090	0.4826	1.26	1.368	0.1426			

2.4.4. Calibration and validation of SWAT model for the whole ZRB

A reasonable prediction of runoff generation from the SWAT watershed was ensured by calibrating the SWAT model for the whole ZRB. For this purpose, the ZRB was subdivided into 12 sub-watersheds (Fig. 5). Fig. 5 also shows the Thiessen polygons used to determine the areal average rainfall for each sub-watershed and that sub-watershed 6 is the same as the SWAT watershed shown in Fig. 3. The SWAT model for the ZRB consisted of 520 HRUs produced by overlaying soil map, land use map and five slope classes (0–5, 5–10, 10–15, 15–20, and 20–9999%) using threshold values of 5, 5 and 5% for land use, soil, and slope classes, respectively. The observed record was split into calibration period (January 1st, 1986–December 31st, 2000), validation period (January 1st, 2001, December 31st, 2010) and warm-up period (January 1st, 1984 to December 31st, 1985). The parameters selected for calibration include curve number (CN), AWC, plant uptake compensation factor (EPCO), soil evaporation compensation factor (ESCO), slope length, baseflow recession constant (ALPHA_BF), and surface runoff lag time (SURLAG). The ALPHA_BF and SURLAG were calibrated on the basin level, while all the other parameters were calibrated on the HRU level.

2.5. HYDRUS model

2.5.1. General description

HYDRUS uses two constitutive functions to describe unsaturated hydraulic conditions: the traditional single porosity (SP) function of VG (van Genuchten, 1980), and a DP derivation of VG (Durner et al., 1999). Both functions are applicable to the HYDRUS 3D domain. The original VG equation (1980) (SP) is

$$\theta(h) = \theta_r + \frac{\theta_s - \theta_r}{[1 + |\alpha h|^n]^m} \tag{5}$$

where θ_s is the saturated water content (m^3/m^3), θ_r is the residual soil water content (m^3/m^3), α (m/day), m, and n are fitting (empirical) parameters, with $m = 1 - 1/n$.
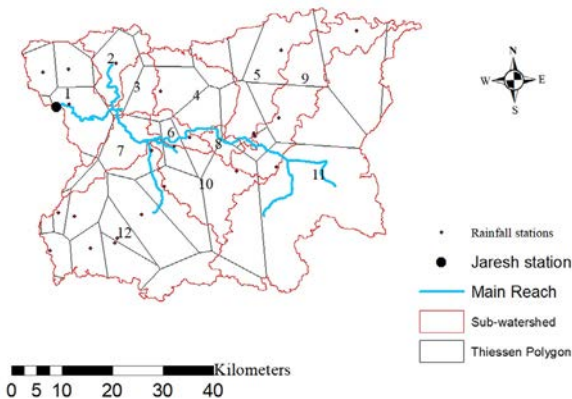
Fig. 5. Setup of Soil and Water Assessment Tool (SWAT) model for the Zarqa River Basin. The basin was divided to 12 sub-watersheds. Thiessen polygons were used to determine the average areal rainfall for each sub-watershed.

The unsaturated conductivity is determined according to the following VG function (SP):

$$K(h) = K_s S_e^l \left[1 - \left(1 - S_e^{1/m}\right)^m\right]^2 \tag{6}$$

where S_e is the effective water content, K_s is the saturated hydraulic conductivity (m/day), and $K(h)$ is the hydraulic conductivity at matric potential h (m/day).

Durner et al. (1999) extended the VG function into a DP function as follows:

$$S_e = w_1[1 + (\alpha_1 h)^{n_1}]^{-m} + w_2[1 + (\alpha_2 h)^{n_2}]^{-m_2} \tag{7}$$

$$K(S_e) = K_s \frac{(w_1 S_e + w_2 S_e)^l \left(w_1 \alpha_1 \left[1 - \left(1 - S_e^{1/m}\right)^m\right] + w_2 \alpha_2 \left[1 - \left(1 - S_e^{1/m}\right)^m\right]\right)^2}{(w_1 \alpha_1 + w_2 \alpha_2)^2} \tag{8}$$

where w_1 and w_2 are weighting factors for the overlapping regions. The subscripts 1 and 2 denote region 1 and region 2, respectively.

2.5.2. Setup

2.5.2.1. Geometric configuration. The geometric configuration of the HYDRUS 3D domain was established from contour lines with 1-m intervals interpolated from the 30 m Digital Elevation Model (DEM) acquired from Landsat. The terrain was then digitized and transferred to HYDRUS. The domain was split geometrically into two subdomains representing the Aydoun and Ramtha soil types. Subsequently, each subdomain was divided into three layers. The total soil profile depth of the Aydoun and Ramtha soil was 142 and 86 cm, respectively. The surface layer was set to a depth of 32 cm for both domains, but the remaining depth of the soils was divided equally into the second and third layers. Thus, the depth of the second and third layers depended on the total depth of the soil profile and the vertical discretization of the two soil profiles was 32, 55, 55 cm, and 32, 27, 27 cm for the Aydoun and Ramtha soils, respectively (Table 2).

2.5.2.2. Finite element mesh and time discretization. The mesh was created using a triangular prism elements with a uniform size of 18 m. Thus, the mesh consisted of 26,060 nodes and 76,033 elements. HYDRUS uses variable time steps that maintain numerical stability and ensure efficient use of the CPU. The HYDRUS time algorithm requires the specification of the initial, minimum and maximum time steps, which were set to values of 10^{-5}, 10^{-6} and 5 days, respectively.

2.5.2.3. Boundary conditions. Three types of boundary conditions were applied to the HYDRUS site:

1. Atmospheric boundary condition, which allows rainfall and evapotranspiration simultaneously from the same nodes. The potential evapotranspiration estimates of the SWAT model were used as input data for the HYDRUS model. Potential evapotranspiration estimates were split into potential evaporation and potential transpiration based on the estimated leaf area index. The rainfall

was combined with irrigation events previously predicted by SWAT.

2. Free boundary condition imposed on the base layer. This boundary condition assumes that the water table is far below the bottom boundary. The percolation is calculated based on a zero-pressure head gradient.

3. Seepage face boundary condition imposed on the side boundary along the foot slope of the domain.

2.5.2.4. Initial conditions. Each simulation year started on January 1st when evapotranspiration rates are low and soil water contents are near field capacity. Soil water was initiated at field capacity, which was implemented in HYDRUS by setting the initial soil water potential to −350 cm. This was confirmed by a quick examination of the SWAT HRU output file, which also indicated that soil water was near capacity at the beginning of each simulation year.

2.5.3. Parameterization

The in situ tension infiltrometer measurements were conducted at three locations within the HYDRUS site, representing the shoulder, back and foot slopes. The parameters of the DP function of the surface layer were deduced by performing inverse solution on the in situ tension infiltrometer measurements, while the parameters of the SP function (Eq. (6)) for all layers were deduced from the sand, silt, and clay fractions using the neural network prediction tool included in HYDRUS. Satisfactory inverse solutions were obtained for the surface layer and the sublayers of the shoulder and back slope sites (Table 2). However, both the SP and DP functions led to unsatisfactory inverse solutions at the foot slope sites. For that site, reasonable fit between the simulated and calibrated data was obtained by manually calibrating the dual permeability model. Unfortunately, HYDRUS accommodates the dual permeability model only in the two-dimensional (2D) context; therefore, the results of the foot slope were not included in the three-dimensional characterization of the site. The final set of parameters was used to parameterize the HYDRUS DP and HYDRUS SP models (Table 2). The subsurface layers in both models were represented by the

SP function, while the DP function was applied to the surface layer of the HYDRUS DP model.

For the HYDRUS SP and HYDRUS DP models, the distribution of the root water uptake calculated by Eq. (4) was edited into the HYDRUS soil properties table in order to allow for root uptake conditions similar to the SWAT model.

3. Results

3.1. SWAT model

3.1.1. Calibration and validation

The curve numbers (CNs) for the HRUs involved were kept at their default values: 81 for Aydoun and 78 for Ramtha. Runoff generation simulated by SWAT was near zero in 1990 and 1993, and 6 and 22 mm of runoff were generated during 1991 and 1992, respectively (Fig. 6). This seems reasonable considering the available knowledge of the SWAT watershed. For example, visual observations made by landowners and farmers suggest that runoff is either non-existing or minimal, thus major runoff events are not anticipated. The low runoff in the SWAT watershed (Fig. 3) was also verified by calibrating and validating SWAT for the whole ZRB. The comparison between streamflow simulated by SWAT and observed streamflow at the Jaresh bridge station (Fig. 5) yielded acceptable Nash-Sutcliffe coefficients of 0.70 and 0.62 for the calibration and validation periods, respectively (Figs. 7 and 8). Fig. 9 shows the areal average rainfall of each sub-watershed during the four-year simulation period (1990–1993). The annual average runoff from the SWAT watershed (Fig. 3) was about 4.7 mm, which is close to the 5.7 mm simulated by the SWAT model calibrated for the whole ZRB area (Fig. 10).

3.1.2. Irrigation schedule

The irrigation schedule was predicted by SWAT using the automatic irrigation practice option, which was set to restore the soil water content (SWC) to field capacity (FC) after 20 mm depletion of SWC. The irrigation schedules simulated by SWAT for each HRU within the HYDRUS site
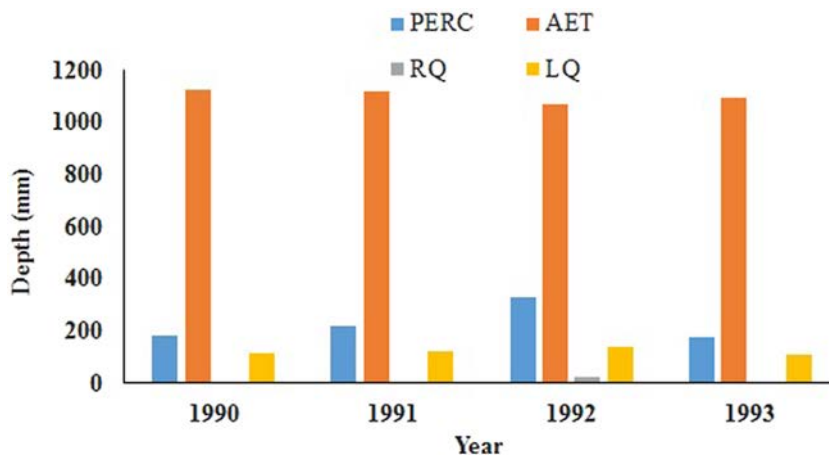

Fig. 6. SWAT output within the HYDRUS site. The results are for the calendar years 1990, 1991, 1992, and 1993. PERC is the annual deep percolation (mm), AET is the annual actual evapotranspiration (mm), RQ is the annual runoff (mm), and LQ is the annual lateral discharge (mm).
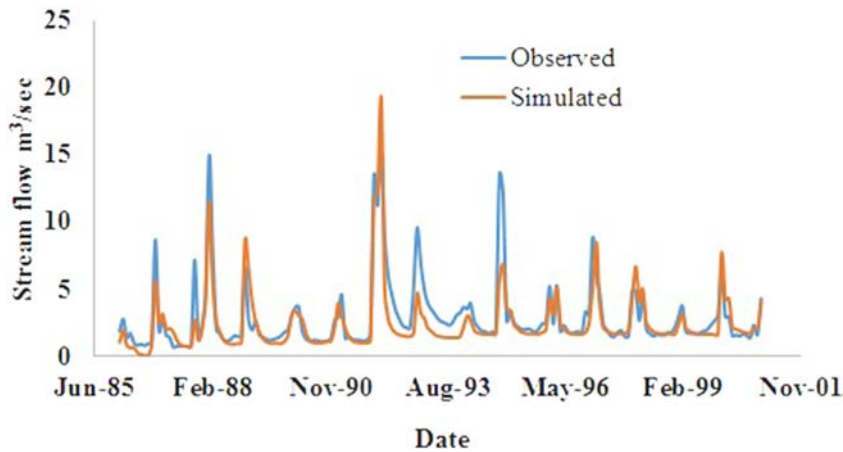
Fig. 7. Comparison between observed and simulated average monthly stream flow during the calibration period of January 1986 to December 2000. The stream flow was measured at Jaresh bridge station. The Nash-Sutcliffe Efficiency for the calibration period was 0.70.
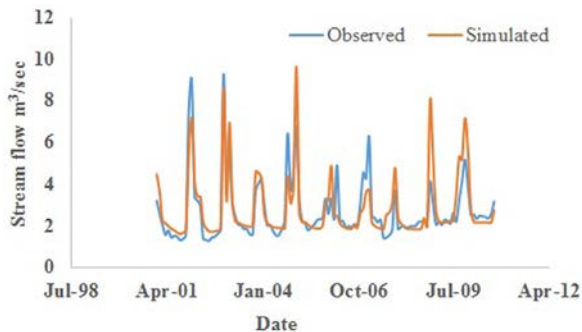

Fig. 8. Comparison between observed and simulated average monthly stream flow during the validation period of January 2001 to December 2010. The stream flow was measured at Jaresh bridge station. The Nash-Sutcliffe Efficiency for the validation period was 0.62.

were similar but not identical. For example, the cumulative irrigation depths simulated by SWAT during the calendar year of 1993 were between 940 and 1280 mm (Fig. 11). A record low rainfall of 47 mm (Fig. 4) was observed during 1993. Therefore, a cumulative irrigation depth of 1280 mm simulated by SWAT for the Ramtha/15-999 HRU during 1993 would reasonably account for the crop water requirement for all seven HRUs located within the HYDRUS site (Table 3). Hence, a fixed irrigation schedule was adopted in order to facilitate similar irrigation schedules for SWAT and HYDRUS.

3.1.3. Soil water

SWAT estimated area weighted average actual evapotranspiration rates of 1128, 1117, 1070 and 1094 mm, for the calendar years of 1990, 1991, 1992, and 1993, respectively (Fig. 12). Water stress was not indicated in any of the HRUs, hence the fixed irrigation schedule was adequate and enough water was supplied to the crops.

The area weighted average of the percolation depth simulated by the SWAT model showed that deep percolation was induced by daily rainfall greater than 20 mm (Fig. 13). Approximately one third of total deep percolation was influenced by rainfall events during 1991 and 1993,

the years that saw near and above average annual rainfall, respectively. A steady increase in deep percolation was simulated during the dry summer season as the result of the fixed irrigation schedule that tends to keep the soil water content slightly above field capacity. SWAT results also suggested that deep percolation is influenced by slope class (Fig. 14). The percolation values of the 0–5, 5–10 and 10–15% slope classes oscillated around the area weighted average, but the excess soil water from the 15–9999% slope class was removed from the soil profile via subsurface lateral flow. SWAT predicted an annual lateral flow between 108 and 140 mm, which was not simulated by the SP and DP HYDRUS models.

Two SWAT parameters were adjusted in order to eliminate the discrepancy between SWAT and DP, ESCO and the slope length parameter. ESCO is defined as the evaporation soil compensation factor and was initially set to a default value of 0.95, which only allows evaporation to occur from the top 100 mm of the soil. During calibration, ESCO was reduced to a value of 0.8 to allow SWAT to meet the evaporative demand from the upper 200 mm of the soil profile. The reduction of the ESCO parameter resulted in a net decrease in deep percolation as more soil water was extracted to meet the evaporation demand. The slope length is the subsurface length used in SWAT for the calculation of lateral discharge. A short slope length means that most of the soil water saturating the lower, semi-impermeable soil layer will be discharged to the main stream as lateral flow. To reduce the lateral discharge simulated by SWAT, the slope length was set to an upper limit value of 150 m. Thereby 90% of the lateral flow simulated by SWAT was eliminated (Fig. 13). Overall, the gap between the SWAT and the HYDRUS DP models was narrowed by calibrating ESCO and the slope length.

3.2. HYDRUS model

3.2.1. Soil water

The SWAT results were contrasted with two HYDRUS simulations. The first simulation assumed no preferential flow, so the soil physical properties were characterized by
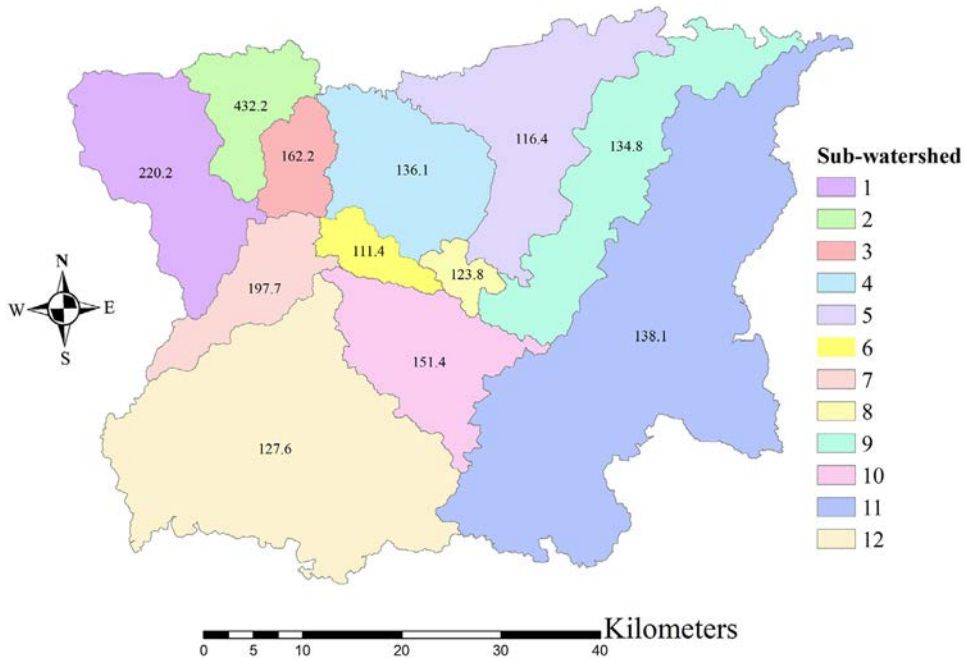
Fig. 9. Four year (1990–1993) average areal rainfall depth (mm) for each sub-watershed within the Zarqa River Basin.
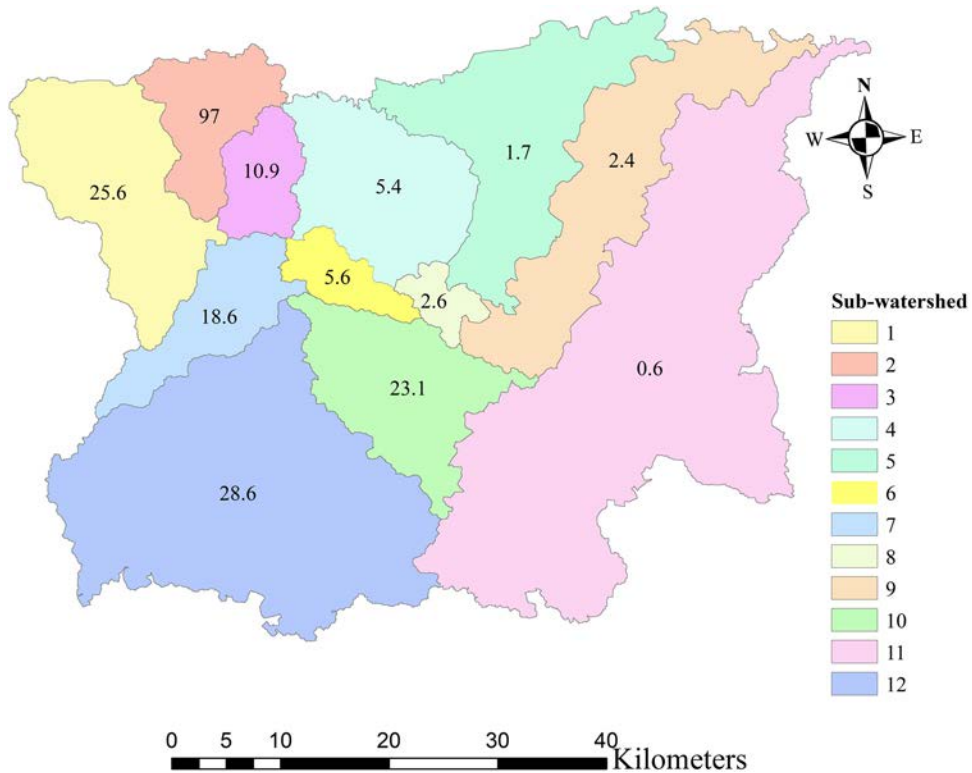

Fig. 10. Four year (1990–1993) average of runoff depth (mm) from each sub-watershed within the Zarqa River Basin.

the SP model. For the second HYDRUS simulation, preferential flow was considered by using the DP model (Table 2). The cumulative flux from the free drainage boundary condition for both HYDRUS simulations reiterated the general deep percolation pattern found in SWAT results, especially the peaks of deep percolation induced by substantial rainfall events (Fig. 13). The total deep percolation simulated by the SP model was approximately half the deep percolation
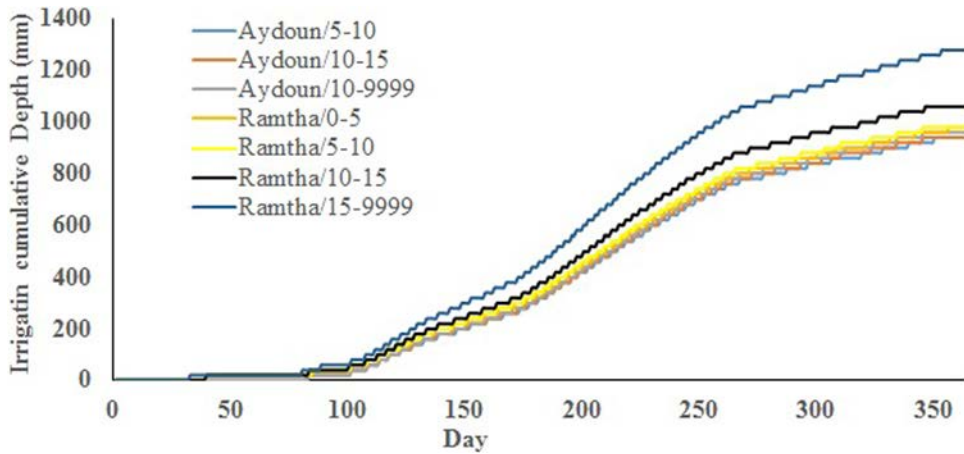
Fig. 11. Cumulative irrigation depth simulated by SWAT for the seven HRUs encountered within the HYDRUS site.

Table 3
The area fraction of each Hydrologic Response Unit (HRU) contained within the HYDRUS for numerical modeling.

HRU	Aydoun			Ramtha			
	5–10	10–15	15–999	0–5	5–10	10–15	15–999
Area fraction	0.01	0.03	0.32	0.09	0.2	0.09	0.24

simulated by the DP model. However, for the calendar year of 1992, the SP model simulated 200 mm of deep percolation, i.e. two thirds of the deep percolation predicted by the DP model. This was due to the above average rainfall during 1992. The SP model demonstrated a gradual decrease in the percolation rates and a smooth response to major rainfall events.

In contrast, HYDRUS DP and SWAT models demonstrated abrupt increases in the cumulative percolation rates, which coincided with major rainfall events. For example, percolation rates spiked at Julian days 334 in 1991 and 33 in 1992. SWAT-simulated annual percolation
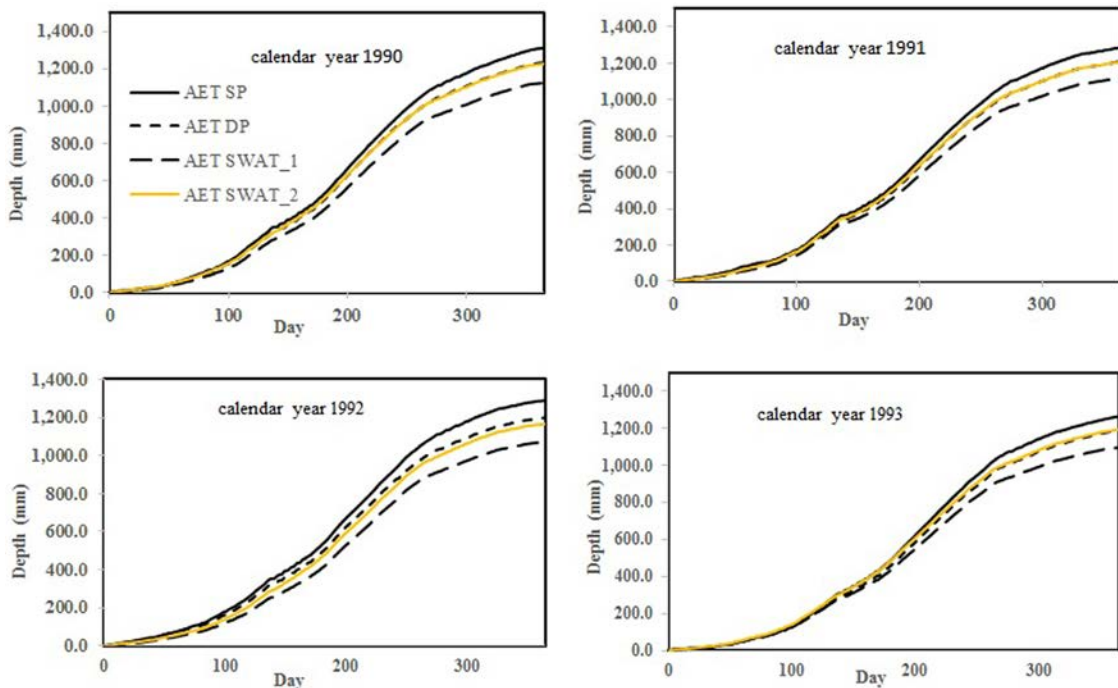

Fig. 12. Comparison between SWAT, HYDRUS dual porosity (DP), and HYDRUS single porosity (SP) simulations of actual evapotranspiration. AET SP is the HYDRUS single porosity model simulation of AET (mm). AET DP is the HYDRUS dual porosity model simulation of AET (mm). AET SWAT_1 is the SWAT model simulation of AET (mm) with ESCO = 0.95 and default slope length. AET SWAT_2 is the SWAT model simulation of lateral flow (mm) with ESCO = 0.80 and slope length is 150 m.
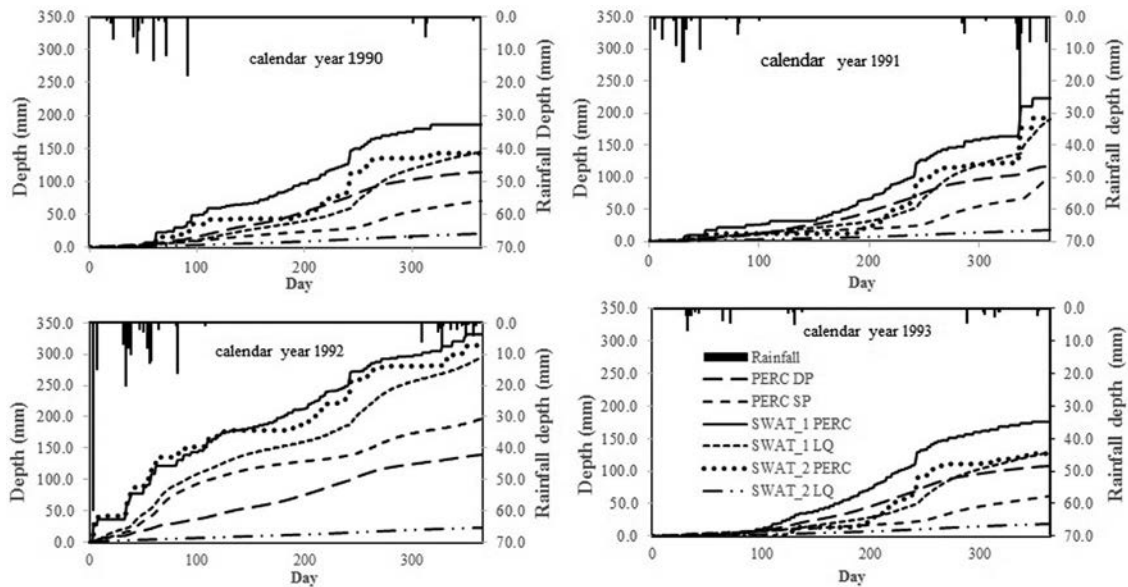
Fig. 13. Comparison between SWAT, HYDRUS dual porosity (DP), and HYDRUS single porosity (SP) simulations of cumulative deep percolation and cumulative lateral discharge. PERC DP is the HYDRUS dual porosity model simulation of cumulative deep percolation (mm). SWAT_1 PERC is the SWAT model simulation of deep percolation (mm) with ESCO = 0.95 and average slope length 12 m. SWAT_1 LQ is the SWAT model simulation of lateral flow (mm) with ESCO = 0.95 and default slope length. SWAT_2 PERC is the SWAT model simulation of deep percolation (mm) with ESCO = 0.80 and slope length 150 m. SWAT_2 LQ is the SWAT model simulation of lateral flow (mm) with ESCO = 0.80 and slope length 150 m.
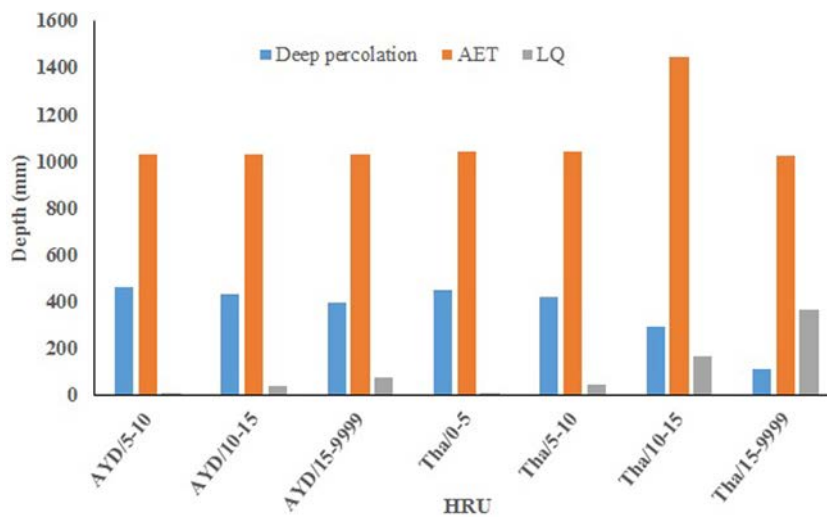

Fig. 14. SWAT output of each HRU within the HYDRUS site. The results are for the calendar year of 1992. PERC is annual deep percolation (mm), AET is the annual actual evapotranspiration (mm), RQ is the annual runoff (mm), and LQ is the annual lateral discharge (mm). AYD and Tha denote Aydoun and Ramtha soils. Each HRU is defined by soil_name/slope_category.

exceeded annual percolation simulated by the HYDRUS DP model by an average of 40 mm.

Lateral flow from the seepage boundary conditions was not simulated by the SP or the DP model. Lateral flow through the side boundary only occurs when the seepage boundary is saturated, i.e. the soil water potential is zero. This condition was not met during the simulation period.

The SP model estimated a four year average of 1200 mm of actual evapotranspiration (AET), compared to 1120 and 1045 mm of AET simulated by the DP and SWAT models, respectively (Fig. 13). Thus, the difference in cumulative

percolation between the SP and DP models was partially compensated by a comparable increase in AET.

4. Discussion

4.1. Influence of preferential flow

The DP model was applied to the surface layer. The physical parametrization of this layer was based on in situ field measurements using a tension infiltrometer. Although the subsurface layers were represented by the SP

model, the flow within the soil profile was a function of preferential flow occurring in the surface layer. The fast drainage of soil water from the surface to the subsurface layer reduced the amount of water available to meet the evaporative demand and subsequently increased the deep percolation. This was evident from the comparison of the SP and the DP models. Rahbeh et al. (2013) discussed the role of evapotranspiration in controlling runoff and deep percolation rates. Irrigation can boost crop growth, which increases the evapotranspiration, but the presence of preferential pathways within the surface layer may provide quick release routes for the soil water, which may prompt farmers to add more water. HYDRUS simulations also showed that the differences in the deep percolation simulation between the SP and DP models occurred during the rainy season and was particularly associated with major rainfall events with depths greater than 20 mm. Similarly, Gish et al. (2004) suggested that preferential flow may be initiated by a critical input flux. McGrath et al. (2010) also found that preferential flow is triggered by major rainfall events.

4.2. Implications for the SWAT model

The SWAT model predicted more rapid percolation than the HYDRUS SP and DP models. This can be attributed to the structure of the soil water routing equation in SWAT (Eq. (2)), which approximates the total percolation time based on the saturated hydraulic conductivity (Eq. (3)) without adjusting for unsaturated conditions. Therefore, SWAT not only overestimates the deep percolation rates, but it also alters the hydrological pathways by reducing evaporation from the depleted surface layer and redirecting water from evaporation to deep percolation. Therefore, it is important to adjust the total amounts of deep percolation with respect to evaporation. This may be done by reducing the ESCO parameter to 0.8 or less, which extends the subsurface depth from which the evaporative demand can be met, thus at least partially restricting the rapid downward movement of soil water.

The soil water in excess of field capacity may become lateral discharge if the horizontal saturated water movement exceeds the percolation rate through the bottom soil layer. This condition was simulated by SWAT for HRUs characterized by steep slopes, where rapid downward movement of soil water caused an overestimation of lateral discharge. The results of the HYDRUS models showed that subsurface layers never reached saturation, so lateral discharge was not simulated by either the SP or the DP models. Besides the saturated hydraulic conductivity, the lateral discharge in SWAT is also governed by the soil slope length. A short slope length means fast removal of excess soil water via the lateral discharge route. However, on a typical hillslope there is a gradual transition between steep (shoulder) and gentle (foot) slopes. Furthermore, the actual discharge of lateral flow occurs at the interface of the stream and the foot slope. It is not possible to measure the actual length of the soil slope in SWAT because the HRUs are not geo-referenced within each sub-watershed. Therefore, the length of the soil slope should be considered as a parameter that can be adjusted in order to alter the

subsurface water movement from horizontal to vertical directions. This is especially justified in arid watersheds, where the lack of vertical saturation of the soil profile prevents the initiation of horizontal water movement.

4.3. The combined use of HYDRUS and SWAT models

The comparison between the results of HYDRUS and SWAT models provided two benefits for this research. The first benefit is that the HYDRUS model provided a better physical interpretation of the SWAT model results. The results suggested that the SWAT model resembles the HYDRUS DP model, indicating that the SWAT model already contains some aspects of preferential flow. Such an outcome is favorable for this research because the in situ soil measurements conducted along the Zarqa River strongly suggested the presence of preferential flow. For other case studies where matrix flow prevails, the HYDRUS model can be used to address and verify necessary improvements in the SWAT model, such as adjusting the soil water routing module (Eqs. (2) and (3)) for unsaturated conditions. It is noteworthy that SWAT model simulations of deep percolation and groundwater recharge may be difficult to verify using the standard calibration and validation process (Rahbeh et al., 2011). In this regard, the HYDRUS model can provide an additional verification of SWAT model results.

The second benefit is that the HYDRUS model helped in narrowing the range of values for two SWAT parameters, ESCO and the soil slope length. The standard calibration and validation approach of the SWAT model produces several combinations of calibrated parameters that can provide a satisfactory fit between the simulated and the observed data. However, several possible sets of calibrated parameters may also lead to contradictory conclusions. The HYDRUS model can help in selecting the most plausible set of calibrated parameters.

5. Conclusion

The in situ measurements using a tension infiltrometer and the results of the HYDRUS DP model showed that preferential flow processes occurring in the upper 30 cm of the soil profile control the downward movement of excess soil water.

Both the SWAT and HYDRUS DP models are suitable for predicting preferential soil water movement in arid watersheds. In fact, the deep percolation simulations obtained from SWAT resemble the results of the DP model provided that proper parameterization is applied. The ESCO parameter should be set to a value of 0.8 or less. The soil slope length should be set to its maximum possible value (i.e. 150 m) or adjusted to reflect realistic simulation of lateral discharge.

The research results imply that the soil water module of the SWAT model (Eqs. (2) and (3)) requires further consideration because it cannot accommodate the matrix flow.

This research recommends using HYDRUS model to verify SWAT model predictions of soil water redistribution in the soil profile and to improve the parameterization of

the SWAT model. The research also suggests an approach for the combined use of both models including the following basic steps:

1. Select a site or sites within the study watershed for the setup of HYDRUS model.
2. Conduct an initial calibration and validation of the SWAT model for the whole watershed.
3. Select a sub-watershed or sub-watersheds that include the HYDRUS model site or sites and prepare the setup of the SWAT model for the selected sub-watersheds. The sub-watersheds should be small enough to accommodate HRU(s) that have management practices, land use and soil properties similar to the HYDRUS model site(s).
4. Adjust the soil properties values of the SWAT model at the HRU level according to the HYDRUS model results.

Conflict of interest

None declared.

Ethical statement

Authors state that the research was conducted according to ethical standards.

Acknowledgement

References

Ahn, S., Abudu, S., Sheng, Z., Mirchi, A., 2018. Hydrologic impacts of drought-adaptive agricultural water management in a semi-arid river basin: case of Rincon valley, New Mexico. Agric. Water Manag. 209, 206–218, http://dx.doi.org/10.1016/j.agwat.2018.07.040.

Al Kuisi, M., Mashal, K., Al-Qinna, M., Abu Hamad, A., Margana, A., 2014. Groundwater vulnerability and hazard mapping in an arid region: case study, Amman-Zarqa Basin (AZB)-Jordan. J. Water Resour. Prot. 6, 297–318, http://dx.doi.org/10.4236/jwarp.2014.64033.

Al-Bakri, J., Salahat, M., Suleiman, A., Suifan, M., Hamdan, M.R., Khresat, S., Kandakji, T., 2013. Impact of climate and land use changes on water and food security in Jordan: implications for transcending 'The Tragedy of the Commons'. Sustainability 5 (2), 724–748, http://dx.doi.org/10.3390/su5020724.

Al-wadaey, A., Ziadat, F., Oweis, T., Elkhboli, M., Alboueichi, A., 2016. Targeting sub-watersheds with conservation practices using SWAT Model and GIS techniques in Libya. Biosci. Biotechnol. Res. Asia 13 (3), 1353–1362, http://dx.doi.org/10.13005/bbra/2276.

Ankeny, M.D., Kaspar, T.C., Horton, R., 1988. Design for an automated tension infiltrometer. J. Soil Sci. Soc. Am. 5, 893–896, http://dx.doi.org/10.2136/sssaj1988.03615995005200030054x.

Antonopoulos, V.Z., Georgiou, P.E., Kolotouro, C.A., 2013. Soil water dynamics in cropped and uncropped fields in northern Greece using a dual-permeability model. Hydrol. Sci. J. 58 (8), 1748–1759, http://dx.doi.org/10.1080/02626667.2013.816424.

Arnold, J.G., Srinivasan, R., Muttiah, R.S., Williams, J.R., 1998. Large area hydrologic modeling and assessment part I: model development. J.

Am. Water Resour. Assoc. 34 (1), 73–79, http://dx.doi.org/10.1111/j.1752-1688.1998.tb05961.x.

Awan, K.U., Ismaeel, A., 2014. A new technique to map groundwater recharge in irrigated areas using a SWAT model under changing climate. J. Hydrol. 519, 1368–1382, http://dx.doi.org/10.1016/j.jhydrol.2014.08.049.

Bajjali, W., Al-Hadidi, K., Ismail, M., 2017. Water quality and geochemistry evaluation of groundwater upstream and downstream of the Khirbet Al-Samra wastewater treatment plant/Jordan. Appl. Water Sci. 7, 53–69, http://dx.doi.org/10.1007/s13201-014-0263-x.

Bordoni, M., Bittelli, M., Valentino, R., Chersich, S., Meisina, C., 2017. Improving the estimation of complete field soil water characteristic curves through field monitoring data. J. Hydrol. 552, 283–305, http://dx.doi.org/10.1016/j.jhydrol.2017.07.004.

Brooks, R.H., Corey, A.T., 1964. Hydraulic properties of porous media. In: Hydrology. Paper No. 3. Colorado State Univ., Fort Collins, CO.

CFSR. Climate Forecast System Reanalysis (accessed April 2014).

Cho, J., Bosch, D., Lowrance, R., Strickland, T., Vellidis, G., 2009. Effect of spatial distribution of rainfall on temporal and spatial uncertainty of SWAT output. Trans. ASABE 52 (5), 1545–1556, http://dx.doi.org/10.13031/2013.29143.

Cong, Z., Lu, H., Ni, G., 2014. Simplified dynamic method for field capacity estimation and its parameter analysis. Water Sci. Eng. 7 (4), 351–362, http://dx.doi.org/10.3882/j.issn.1674-2370.2014.04.001.

Durner, W., Priesack, E., Vogel, H.J., Zurmühl, T., 1999. Determination of parameters for flexible hydraulic functions by inverse modeling. In: van Genuchten, M.Th., Leij, F.J., Wu, L. (Eds.), Characterization and Measurement of the Hydraulic Properties of Unsaturated Porous Media. University of California, Riverside, CA, pp. 817–829.

Gassman, P.W., Reyes, M.R., Green, C.H., Arnold, J.G., 2007. The soil and water assessment tool: historical development, applications, and future research directions. Trans. Am. Soc. Agric. Biol. Eng. 50 (4), 1211–1250, http://dx.doi.org/10.13031/2013.23637.

Gish, T.J., Kung, K.J.S., Perry, D.C., Posner, J., Bubenzer, G., Helling, C.S., Kladivko, E.J., Steenhuis, T.S., 2004. Impact of preferential flow at varying irrigation rates by quantifying mass fluxes. J. Environ. Qual. 33, 1033–1040, http://dx.doi.org/10.2134/jeq2004.1033.

Hardie, M.A., Cotching, W.E., Doyle, R.B., Holz, G., Lisson, S., Mattern, K., 2011. Effect of antecedent soil moisture on preferential flow in texture-contrast soil. J. Hydrol. 398, 191–201, http://dx.doi.org/10.1016/j.jhydrol.2010.12.008.

Hartwich, J., Schmidt, M., Bölscher, J., Reinhardt-Imjela, C., Murach, D., Schulte, A., 2016. Hydrological modelling of changes in the water balance due to the impact of woody biomass production in the North German Plain. Environ. Earth Sci. 75, 1071, http://dx.doi.org/10.1007/s12665-016-5870-4.

Hatiye, S.D., Kotnoor, H.P.S.R., Ojha, C.S.P., 2017. Study of deep percolation in paddy fields using drainage-type lysimeters under varying regimes of water application. ISH J. Hydraul. Eng. 23 (1), 35–48, http://dx.doi.org/10.1080/09715010.2016.1228086.

Hu, Q., Yang, Y., Han, S., Yang, Y., Ai, Z., Wang, J., Ma, F., 2017. Identifying changes in irrigation return flow with gradually intensified water-saving technology using HYDRUS for regional water resources management. Agric. Water Manag. 194, 33–47, http://dx.doi.org/10.1016/j.agwat.2017.08.023.

Li, H., Yi, J., Zhang, J., Zhao, Y., Si, B., Hill, R.L., Cui, L., Liu, X., 2015. Modeling of soil water and salt dynamics and its effects on root water uptake in Heihe Arid wetland, Gansu, China. Water 7, 2382–2401, http://dx.doi.org/10.3390/w7052382.

McGrath, G.S., Hinz, C., Sivapalan, M., Dressel, J., Pütz, T., Vereecken, H., 2010. Identifying a rainfall event threshold triggering herbicide leaching by preferential flow. Water Resour. Res. 46, W02513, http://dx.doi.org/10.1029/2008WR007506.

Ministry of Agriculture (MOA), 1994. National Soil Map and Land Use Project: The Soils of Jordan. Amman, Jordan.

Musau, J., Sang, J., Gathenya, J., Luedeling, E., 2015. Hydrological responses to climate change in Mt. Elgon watersheds. J. Hydrol.: Reg. Stud. 3, 233–246, http://dx.doi.org/10.1016/j.ejrh.2014.12.001.

Narsimlu, B., Gosain, A.K., Chahar, B.R., 2013. Assessment of future climate change impacts on water resources of Upper Sind River Basin, India Using SWAT Model. Water Resour. Manag. 27, 3647–3662, http://dx.doi.org/10.1007/s11269-013-0371-7.

Neitsch, S.L., Arnold, J.G., Kiniry, J.R., Williams, J.R., King, K.W., 2002. Soil and Water Assessment Tool Theoretical Documentation. Texas Water Resources Institute, College Station, TX 458 pp.

Neupane, R.P., Kumar, S., 2015. Estimating the effects of potential climate and land use changes on hydrologic processes of a large agriculture dominated watershed. J. Hydrol. 529, 418–429, http://dx.doi.org/10.1016/j.jhydrol.2015.07.050.

Neupane, R.P., White, J.D., Alexander, S.E., 2015. Projected hydrologic changes in monsoon-dominated Himalaya Mountain basins with changing climate and deforestation. J. Hydrol. 525, 216–230, http://dx.doi.org/10.1016/j.jhydrol.2015.03.048.

Ouessar, M., Bruggeman, A., Abdelli, F., Mohtar, R.H., Gabriels, D., Cornelis, W.M., 2009. Modelling water-harvesting systems in the arid south of Tunisia using SWAT. Hydrol. Earth Syst. Sci. 13, 2003–2021, http://dx.doi.org/10.5194/hess-13-2003-2009.

Rahbeh, M., Chanasyk, D.S., Miller, J., 2011. Two-way calibration-validation of SWAT model for a small prairie watershed with short observed record. Can. Water Resour. J. 36 (3), 247–270, http://dx.doi.org/10.4296/cwrj3603884.

Rahbeh, M., Chanasyk, D., Miller, J., 2013. Modelling the effect of irrigation on the hydrological output from a small prairie watershed. Can. Water Resour. J. 38 (4), 280–295, http://dx.doi.org/10.1080/07011784.2013.849856.

Shang, F., Ren, S., Yang, P., Li, C., Xue, Y., Huang, L., 2016. Modeling the risk of the salt for polluting groundwater irrigation with recycled water and ground water using HYDRUS-1 D. Water Air Soil Pollut. 227, 189, http://dx.doi.org/10.1007/s11270-016-2875-2.

Sheng, F., Liu, H., Zhang, R., Wang, K., 2012. Determining the active region model parameters from dye staining experiments for characterizing the preferential flow heterogeneity in unsaturated soils. Environ. Earth Sci. 65, 1977–1985.

Šimůnek, J., van Genuchten, M.T., Miroslav, Š., 2016. Recent developments and applications of the HYDRUS computer software packages. Vadose Zone J. 15, 1–25, http://dx.doi.org/10.2136/vzj2016.04.0033.

Taddele, Y., Karlberg, L., Daggupati, P., Srinivasan, R., Wiberg, D., Rockström, J., 2016. Assessing the implications of water harvesting intensification on upstream–downstream ecosystem services: a case study in the Lake Tana Basin. Sci. Total Environ. 542, 22–35, http://dx.doi.org/10.1016/j.scitotenv.2015.10.065.

van Genuchten, M.Th., 1980. A closed form equation for predicting the hydraulic conductivity of unsaturated soils. Soil Sci. Soc. Am. J. 44, 892–898.

Vásquez, V., Thomsen, A., Iversen, B.V., Jensen, R., Ringgaard, R., Schelde, K., 2015. Integrating lysimeter drainage and eddy covariance flux measurements in a groundwater recharge model. Hydrol. Sci. J. 60 (9), 1520–1537, http://dx.doi.org/10.1080/02626667.2014.904964.

Vogel, T., Císlerová, M., 1988. On the reliability of unsaturated hydraulic conductivity calculated from the moisture retention curve. Transp. Porous Media 3, 1–15.

Wang, K., Zhang, R., 2011. Heterogeneous soil water flow and macropores described with combined tracers of dye and iodine. J. Hydrol. 397, 105–117.

Wang, Y., Bradford, S.A., Šimůnek, J., 2014. Estimation and upscaling of dual-permeability model parameters for the transport of E. coli D21g in soils with preferential flow. J. Contam. Hydrol. 159, 57–66.

Wegehenkel, M., Rummel, U., Beyrich, F., 2017. Long-term analysis of measured and simulated evapotranspiration and soil water content. Hydrol. Sci. J. 62 (10), 1532–1550, http://dx.doi.org/10.1080/02626667.2017.1332417.

White, I., Sully, M.J., 1987. Macroscopic and microscopic capillary length and time scales from field infiltration. Water Resour. Res 23 (8), 1514–1522, http://dx.doi.org/10.1029/WR023i008p01514.

Wiekenkamp, I., Huisman, J.A., Bogena, H.R., Lin, H.S., Vereecken, H., 2016. Spatial and temporal occurrence of preferential flow in a forested headwater catchment. J. Hydrol. 534, 139–149.

Wooding, R.A., 1968. Steady infiltration from a shallow circular pond. Water Resour. Res. 4, 1259–1273.

Wu, Q., Wang, G., Zhang, W., Cui, H., Zhang, W., 2016. Estimation of groundwater recharge using tracers and numerical modeling in the North China Plain. Water 8 (353), 1–19.

Xu, X., Kalhoro, S.A., Chen, W., Raza, R., 2017. The evaluation/application of Hydrus-2D model for simulating macro-pores flow in loess soil. Int. Soil Water Conserv. Res. 5, 196–201, http://dx.doi.org/10.1016/j.iswcr.2017.05.010.